

### Computational methods

The calculations are based on first-principles density functional theory. The SIESTA code<sup>1-3</sup> was used to solve the standard Kohn-Sham (KS) equations using numerical atomic orbitals (NAO) basis sets. The local density approximation (LDA) was used for the exchange-correlation term parameterized by Ceperley and Alder.<sup>4</sup> Core electrons are replaced by non-local, standard norm conserving Troullier-Martins pseudopotentials for C, Cu and I.<sup>5-8</sup> The reference electronic configuration, cut-off radius and partial core cut-off radius for all pseudopotentials employed here are tabulated (Table S1). For Cu and I, a partial core correction is necessary to account for nonlinearity of the exchange and correlation potential between core and valence charge densities. Both the Cu and I pseudopotentials were generated with scalar relativistic effects.

Atom		C	Cu	I
Reference		$2s^2 2p^2 3d^0 4f^0$	$3d^{10} 4s^1 4p^0 4f^0$	$5s^2 5p^2 5d^0 4f^0$
Core radius (a.u.)	s	1.25	2.00	1.80
	p	1.25	2.30	1.90
	d	1.25	2.00	3.00
	f	1.25	2.33	2.10
Core cutoff (a.u.)		0.00	3.43	3.50

**Table S1.** Reference configuration and cut-off radii (a.u.) of the pseudopotentials used in this study.

The quality of the pseudopotential was tested comparing the eigenvalues and excitation energies of all-electron calculations on the same series of atomic configurations. The cross-excitation energies for Cu, I and C pseudopotentials were not more than 0.09 eV, 0.04 eV and 0.09 eV respectively indicating the excellent transferability of these pseudopotentials.

The one-electron Kohn-Sham eigenstates were expanded in a basis of strictly localized NAOs.<sup>9</sup> For carbon, a double  $\zeta$  basis set for  $2s$  and  $2p$  valence states and a single  $\zeta$  basis set for  $3d$  were used. For Cu, a double  $\zeta$  basis set for the  $3d$  and  $4s$  and a single  $\zeta$  basis set for  $3p$  orbitals were used. For I, a double  $\zeta$  basis set for the  $5s$ ,  $5p$  and  $6p$  orbitals and a single  $\zeta$  basis set for the  $5d$  and  $6s$  orbitals were used.

Structure optimizations were performed using a conjugate gradient algorithm and the forces on the atoms were obtained from the Hellmann-Feynmann theorem including Pulay corrections. In all optimised structures forces on the atoms were smaller than 0.06 eV/Å and the stress tensor was less than 0.02 GPa. To represent the charge density a cut-off of 200–250 Ry for the real space grid integration was used in all calculations.

The quality of the optimised pseudo potentials and basis sets for Cu and I was tested by performing calculations on bulk CuI (zinc blende structure). A series of single point calculations were performed on CuI as a function of lattice constant to obtain the equilibrium lattice constant and bulk modulus. Reciprocal space was sampled using 32  $\mathbf{k}$ -points; increasing the  $\mathbf{k}$  space sampling regime produced negligible changes in the total energy of the system. The  $\mathbf{k}$  points were generated by using Monkhorst-Pack method.<sup>10</sup> The unit cell volume was varied within  $\pm 5\%$  of the equilibrium volume and a cohesive curve was plotted by fitting values of the calculated energy to the Murnaghan equation of state<sup>11,12</sup> Band structure and density of states (DOS) calculations were performed on bulk CuI (ZB) at the equilibrium unit cell volume.

Geometries of 1-d CuI were initially optimised with periodic boundary conditions in the absence of a SWNT from two initial starting points. The lower energy structure was then optimised within three SWNT of differing diameters. A single  $\mathbf{k}$ -point ( $\Gamma$ ) was used for all calculations on 1-d CuI crystals and for the CuI@SWNT composites. For calculations on 1-d CuI crystals and CuI@SWNT composites, periodic boundary conditions were applied to enforce a minimum lateral separation of 25 Å between structures in adjacent unit cells. At this separation the interaction between these structures and their periodic images are negligible. Basis set superposition errors (BSSE) corrections were employed in calculation of all binding energies. Mulliken population charge analysis was carried out to estimate the charge transfer between the CuI crystals and the tubes.

The calculated equilibrium lattice constant for CuI (6.028 Å) and bulk modulus (45.32 GPa), derived from the Murnaghan fit, were in good agreement with the experimental values<sup>13</sup>, and with the results of theoretical calculations (Table S2) thereby validating the choice of pseudopotentials and basis sets.

Parameter	SIESTA	Expt	Other theoretical works
Lattice constant, $a$ (Å)	6.028	6.054 <sup>13</sup>	6.042, <sup>15</sup> 6.051, <sup>16</sup> 6.062, <sup>17</sup> 6.082, <sup>18</sup>
Bulk modulus, $B_0$ (GPa)	45.32	31.0, <sup>19</sup> 36.6 <sup>13</sup>	35.2, <sup>17</sup> 39.7, <sup>18</sup> 58.48 <sup>14</sup>

**Table S2.** Calculated and experimental lattice constants and bulk modulus of CuI zinc blende structure.

The initial structures are shown in Figure S1.

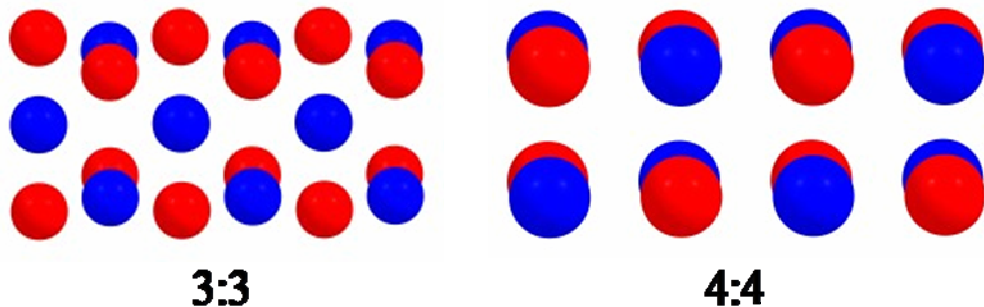


**Figure S1.** Two starting structures proposed for 1-d crystals of CuI with 3:3 and 4:4 coordination (**Cu- blue and I-red**)

Type	$E_{b(unc)}$	$E_{b(CP)}$	$\Delta E_{CuI\_dis}$	$\Delta E_{SWNT\_dis}$	$E_{b(corr)}$
$Cu_{24}I_{24}@ (8,8)$	-0.47	+0.15	+0.10	+0.10	+0.35
$Cu_{24}I_{24}@ (9,9)$	-0.77	-0.18	+0.002	+0.003	-0.17
$Cu_{24}I_{24}@ (10,10)$	-0.44	-0.19	+0.037	+0.009	-0.14

**Table S3.** Uncorrected binding energies,  $E_{b(unc)}$  (eV/CuI), counterpoise corrected binding energies,  $E_{b(CP)}$  (eV/CuI), distortion energy of CuI crystals,  $\Delta E_{CuI\_dis}$  (eV/CuI) and distortion energy of nanotube,  $\Delta E_{SWNT\_dis}$  (eV/CuI) and the corrected binding energy,  $E_{b(corr)}$  (eV/CuI).

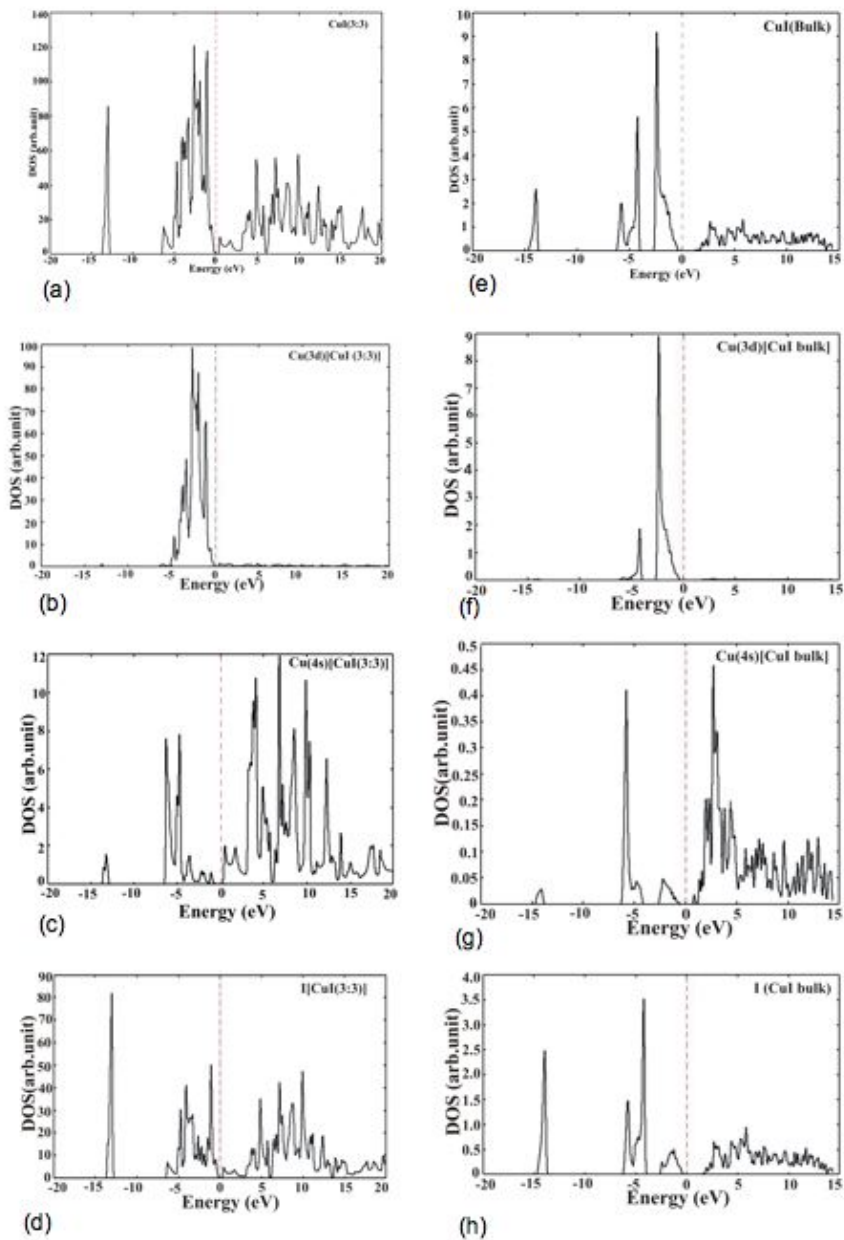


**Figure S2.** Density of states (DOS) and partial density of states (PDOS) for 1-d CuI (a) total (b) Cu 3d (c) Cu 4s (d) I 5s and 5p; DOS and PDOS for bulk CuI. (e) total (f) Cu 3d (g) Cu 4s (h) I 5s and 5p.

Supplementary Material (ESI) for Chemical Communications

This journal is (c) The Royal Society of Chemistry 2008

- (01) P. Ordejon, D. Sanchez-Portal, A. Garcia, E. Artacho, J. Junquera, and J. M. Soler, *RIKEN Review*, 2000, **29**, 42.
- (02) E. Artacho, D. Sanchez-Portal, P. Ordejon, A. Garcia, and J. M. Soler, *Phys. Stat. Sol. B*: 1999, **215**, 809.
- (03) J. M. Soler, E. Artacho, J. D. Gale, A. Garcia, J. Junquera, P. Ordejon, and D. Sanchez-Portal, *J. Phys.: Condens. Matter*, 2002, **14**, 2745.
- (04) D. M. Ceperley and B. J. Alder, *Phys. Rev. Lett.*, 1980, **45** (7), 566.
- (05) D. R. Hamann, M. Schlüter, and C. Chiang, *Phys. Rev. Lett.* 1979, **43**, 1494.
- (06) G. B. Bachelet, M. Schlüter, *Phys. Rev. B* 1982, **25**, 2103.
- (07) M. Fuchs, M. Scheffler, *Comp. Phys. Comm.* 1999, **119**, 67.
- (08) N. Troullier and J. L. Martins, *Phys. Rev. B* 1991, **43**, 1993.
- (09) J. Junquera, O. Paz, D. Sanchez-Portal, E. Artacho, *Phys. Rev. B* 2001, **64**, 235111.
- (10) H.J. Monkhorst, J.D. Pack, *Phys. Rev. B* 1976, **13**, 5188.
- (11) Murnaghan, F.D. *Proc Nat Acad Sci* 1944, **30**, 244.
- (12) M. Bockstedte, A. Kley, J. Neugebauer, M. Scheffler, *Comput. Phys. Commun.* 1997, **107**, 187.
- (13) S. Hull, D.A. Keen, *Phys. Rev. B* 1994, **50**, 5868.
- (14) B. Amrani, T. Benmessabih, M. Tahiri, I. Chiboub, S. Hiadsi, F. Hamdache, *Physica B: Condensed Matter*, 2006, **381**, 179.
- (15) R. W. G. Wyckoff, *Crystal Structures*, vol 1, Wiley, New York.
- (16) C. Schwab, A. Goltzene, *Progr. Crys. Growth*. 1982, **5**, 233.
- (17) W. Sekkal, A. Zaoui, A. Laref, M. Certier, H. Aourag, *J. Phys.: Condens. Matter*. 2000, **12**, 6173.
- (18) F. El Haj Hassan, A. Zaoui, W. Sekkal, *Mater. Sci. Eng B* 2001, **B87**, 40.
- (19) H.L. Hermann, G. Boche, P. Schwerdtfeger, *Phys. Rev. B* 1995, **51**, 12022.